Glycoconj J (2010) 27:159–169
DOI 10.1007/s10719-009-9268-3

N-glycan moieties of the crustacean egg yolk protein and their glycosylation sites

Ziv Roth · Shmuel Parnes · Simy Wiel · Amir Sagi · Nili Zmora · J. Sook Chung · Isam Khalaila

Received: 2 June 2009 / Revised: 23 October 2009 / Accepted: 27 October 2009 / Published online: 18 November 2009

Abstract Vitellogenin (Vg) is the precursor of the egg yolk glycoprotein of crustaceans. In the prawn *Macrobrachium rosenbergii*, Vg is synthesized in the hepatopancreas, secreted to the hemolymph, and taken up by means of receptor-mediated endocytosis into the oocytes. The importance of glycosylation of Vg lies in its putative role in the folding, processing and transport of this protein to the egg yolk and in the fact that the *N*-glycan moieties could provide a source of carbohydrate during embryogenesis. The present study describes, for the first time, the structure of the glycan moieties and their sites of attachment to the Vg of *M. rosenbergii*. Bioinformatics analysis revealed seven putative *N*-glycosylation sites in *M. rosenbergii* Vg; two of these glycosylation sites are conserved throughout the Vgs of decapod crustaceans from the Pleocyemata suborder (N^{159} and N^{660}). The glycosylation of six putative sites of *M. rosenbergii* Vg (N^{151}, N^{159}, N^{168}, N^{614} N^{660} and N^{2300}) was confirmed; three of the confirmed glycosylation sites are localized around the N-terminally conserved *N*-glycosylation site N^{159}. From a theoretical three-dimensional structure, these three *N*-glycosylated sites N^{151}, N^{159}, and N^{168} were localized on the surface of the Vg consensus sequence. In addition, an uncommon high mannose *N*-linked oligosaccharide structure with a glucose cap ($Glc_1Man_9GlcNAc_2$) was characterized in the secreted Vg. These findings thus make a significant contribution to the structural elucidating of the crustacean Vg glycan moieties, which may shed light on their role in protein folding and transport and in recognition between Vg and its target organ, the oocyte.

Keywords Crustacea · Glucose cap · Glycosylation sites · *N*-glycan · Vitellogenin

Abbreviations

ACN	acetonitrile
DIG	digoxigenin
DSA	*Datura stramonium* agglutinin
DTT	dithiothreitol
ER	endoplasmic reticulum
Glc	glucose
GlcNAc	*N*-acetylglucosamine
GII	glucosidase II
GNA	*Galanthus nevallis* agglutinin
GU	glucose unit
HDL	high density lipoprotein
Hex	hexose
HexNAc	*N*-acetylhexosamine
HPLC	high performance liquid chromatography
JBM	jack bean α-mannosidase

Electronic supplementary material The online version of this article (doi:10.1007/s10719-009-9268-3) contains supplementary material, which is available to authorized users.

Z. Roth · I. Khalaila (✉)
Department of Biotechnology Engineering,
Ben-Gurion University of the Negev,
P.O.Box 653, Beer-Sheva 84105, Israel
e-mail: isam@bgu.ac.il

Z. Roth · S. Parnes · S. Wiel · A. Sagi
Department of Life Sciences,
Ben-Gurion University of the Negev,
Beer-Sheva 84105, Israel

Z. Roth · S. Parnes · S. Wiel · A. Sagi
The National Institute for Biotechnology in the Negev,
Ben-Gurion University of the Negev,
Beer-Sheva 84105, Israel

N. Zmora · J. S. Chung
Center of Marine Biotechnology, University of Maryland
Biotechnology Institute,
Baltimore, MD 21202, USA

MAA	*Maackia amurensis* agglutinin
Man	mannose
MALDI	matrix-assisted laser desorption/ionization
PNA	peanut (*Arachis hypogaea*) agglutinin
PNGase F	peptide-*N*-glycosidase F
SDS-PAGE	sodium dodecyl sulfate polyacrylamide gel electrophoresis
SNA	*Sambucus nigra* agglutinin
TFA	trifluoroacetic acid
Vg	vitellogenin

Introduction

Elucidation of the structural modifications of vitellogenin (Vg), a key protein in embryonic development, and understanding the regulatory factors that control its translation, secretion and accumulation are important issues for aquaculture and for pest control. Vg is the precursor of the major yolk protein, vitellin that accumulates in the oocytes of oviparous animals. Vg is synthesized in distinct organs, such as the liver in vertebrates [1] and the fat body in insects [2]. In crustaceans, Vg is synthesized mainly in the hepatopancreas [3–5], from where it is transported by the hemolymph to the Vg storage organ, the ovary. In the ovaries, Vg is sequestered by means of receptor-mediated endocytosis into the oocytes [6–10], where it is packed into mature yolk vesicles that contain the lipoprotein vitellin, lipids and carbohydrates. These yolk vesicles thus supply the nutritional demands of the developing embryos throughout embryonic development until they reach the feed-independent juvenile stage.

There are two conserved domains in the Vg of both vertebrates and invertebrates, the lipid-binding domain at the N-terminal end and the Von Willebrand D domain at the C-terminal end [11]. In decapod crustaceans, the deduced Vg sequence consists of four domains: the lipoprotein domain, two domains of unknown function (designated DUF 1943 and 1081), and the Von Willebrand type D domain (Fig. 1B). Since secretory proteins are shuttled to the oocytes, it is probably true that Vgs are modified upon translation. Indeed, it is known that all vertebrate Vgs are posttranslationally glycosylated and phosphorylated in the endoplasmic reticulum (ER) and the Golgi complex before secretion [11]. The high-molecular-weight Vgs of crustaceans have been characterized as heteromultimeric lipoglycoproteins that possess several putative *N*-glycosylation and *O*-glycosylation sites [12]. Early studies revealed that crustacean Vgs are conjugated to carbohydrates and lipids [13]. In a recent study of the composition of oligosaccharides attached to the Vg of the crayfish *Cherax quadricarinatus*, it was shown that the *N*-glycan moieties of the Vg are composed of monoglucosylated and highly mannosylated glycans, ranging from $Glc_1Man_9GlcNAc_2$ to $Man_5GlcNAc_2$ [14].

In the ER of eukaryotic cells, a $Glc_3Man_9GlcNAc_2$ is attached to the putative *N*-glycosylation sites of secreted proteins, and simultaneously glucosidase I removes the external glucose (α1–2). Thereafter, glucosidase II (GII) cleaves the second glucose (α1–3), and the remaining glucose serves as a quality-control sensor for proper folding of the expressed glycoprotein. Upon correct folding, the glucose cap is removed by GII, and finally the protein is released from the ER. If the glycoprotein is misfolded, it will be re-glucosylated by glucosyltransferase and enter once again to the folding cycle. Eventually the misfolded protein will be sent to the proteasome degradation system [15]. A glucose cap on a secreted glycoprotein is rare, but it has been reported for a small number of proteins, *e.g.*, on human IgE and on avian IgY immunoglobulins [16–19]. There are also reports of a glucose cap on storage glycoproteins, such as arylphorin of the silk worm *Antheraea pernyi* [20] and the egg jelly coat of the starfish, *Asterias amurensis* [21]. Noteworthy, that more than 90%

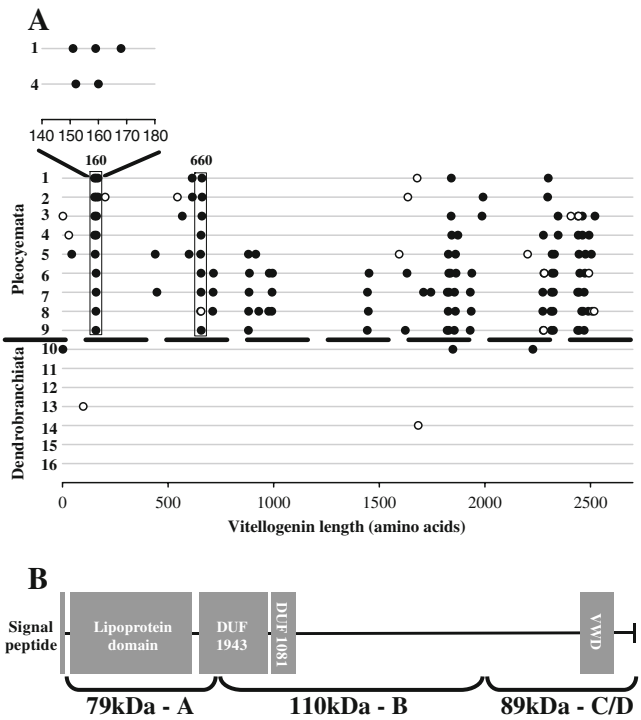

Fig. 1 **A** Distribution of hypothetical *N*- and *O*- glycosylation sites on vitellogenin sequences of decapod crustaceans. Each of the numbered lines represents a sequence from a specific decapod species, and the numbers correspond to the numbering of species names in Table 1. Segregation into two suborders is indicated by the dashed line (above the line - Pleocyemata, below - Dendrobranchiata). Putative *N*-glycosylation sites — black circles; putative *O*-glycosylation sites — hollow circles. **B** Schematic representation of *M. rosenbergii* vitellogenin domains and subunits distribution. DUF — domain of unknown function; VWD — von Willebrand factor type D

of the glycan moieties of arthropods are high-mannose and paucimannose structures [22].

In the current study, we focused on the Vg of the freshwater prawn *Macrobrachium rosenbergii.* The *M. rosenbergii* Vg is composed of four subunits: 79 kDa (subunit A), 110 kDa (subunit B), 89 kDa (subunit C/D) and 199 kDa composed of B and C/D subunits [23]. Structural characterization and modification site analysis of the glycan moieties of Vg are required if we are to understand their role and function in secretion, transport and accumulation. To this end, both bioinformatics and biochemical analyses of the *N*-glycans of Vg from this crustacean species were performed in the current study.

Materials and methods

Materials

Recombinant Peptide-*N*-glycosidase F (PNGase F) (EC 3.5.1.52), Glycan detection kit and Glycan differentiation kit were obtained from Roche diagnostics GmbH (Mannheim, Germany). Trypsin gold mass spectrometry grade was obtained from Promega (Madison, Wisconsin, USA). Jack bean α-mannosidase (JBM) (EC 3.2.1.24) was obtained from Glyko Inc. (Upper Heyford, Oxfordshire, UK). Bradford protein assay kit for determining protein concentration was obtained from Bio-Rad Laboratories GmbH (München, Germany).

Bioinformatics analysis

Vg deduced amino acid sequences of 16 decapod crustaceans were downloaded from the GenBank and searched for *O*- and *N*-glycosylation sites using specific algorithms from the CBS prediction server (http://www.cbs.dtu.dk). *N*-glycosylation sites were determined with NetNGlyc [24] and mucin type *O*-glycosylation sites with NetOGlyc [25]. Names of species and accession numbers are listed in Table 1. The 3D model of the *M. rosenbergii* Vg was created by the ESyPred3D Web server (http://www.fundp.ac.be/sciences/biologie/urbm/bioinfo/esypred) [26] and processed by Swiss-PdbViewer software [27].

Animals and HDL purification

Hemolymph was withdrawn from *M. rosenbergii* secondary vitellogenic females and mixed with 7% EDTA in 1:1 ratio with the addition of 2 mM phenylmethylsulfonyl fluoride (PMSF, Sigma). The solution then centrifuged at 1500 g for 15 min to remove cells and debris. High density lipoprotein (HDL) fractions where isolated as described by Abdu *et al.* (2000) [28] with slight modifications. The hemolymph solution was mixed with a saturated solution of sodium bromide to a density of 1.22 g/ml. HDLs were isolated by ultracentrifugation at 100,000 g for 48 h. The upper golden fraction (HDLs) was collected and dialyzed against 20 mM Tris buffer pH 8.0 and stored at −70°C until further purification.

Chromatography

Hemolymph HDL samples were subjected to two anion-exchange chromatography procedures. The first round of chromatography was performed on a DEAE-Sepharose column (Merck) using NaCl linear gradient (0.1–0.5 M) in 20 mM Tris buffer, pH 8.0. The second round of chromatography was performed on a hydroxyapatite column (Bio-Rad) using linear gradient of 0.1–0.5 M potassium phosphate buffer, pH 7.0. Both steps were performed at a flow rate of 1 ml/min, and absorbance was measured at 280 nm. Fractions of 1 ml were collected, dialyzed, and stored at −70°C. HPLC separated fractions were concentrated by means of lyophilization (Freeze Dry System, LABCONCO). Fractions were analyzed with sodium dodecyl sulfate polyacrylamide electrophoresis (SDS-PAGE), followed by peptide fingerprinting with matrix assisted laser desorption ionization-time of flight-mass spectrometry (MALDI-TOF-MS).

Glycan detection & characterization by lectins

Purified Vg from *M. rosenbergii* was separated on 7% SDS-PAGE and electroblotted onto nitrocellulose membrane. Digoxigenin (DIG) glycan detection kit and DIG glycan differentiation kit were used for glycan detection and structural characterization, respectively. The DIG glycan differentiation kit contains *Galanthus nevallis* agglutinin (GNA), *Sambucus nigra* agglutinin (SNA), peanut (*Arachis hypogaea*) agglutinin (PNA), *Datura stramonium* agglutinin (DSA) and *Maackia amurensis* agglutinin (MAA), which aid in glycan structural characterization.

N-linked glycan analysis and exoglycosidase sequencing

N-linked glycans were released from gel bands of the purified Vg with apparent molecular weights of 199, 110 and 89 kDa, according to the method described by Kuster *et al.* (1997) [29], with slight modifications. Vg was reduced with 55 mM dithiothreitol (DTT) for 10 min at 70°C, before alkylation with 100 mM iodoacetamide at room temperature (protected from light). Thereafter, 15 µg of alkylated Vg was separated on 7% SDS-PAGE and stained with Imperial protein stain (Pierce). After destaining with water, individual protein bands were excised from the gel. The gel pieces were destained with a solution of acetonitrile (ACN): 25 mM $NaHCO_3$ (1:1, v:v). Subsequently, the gel

Table 1 Decapoda vitellogenin sequences analyzed in this study

Line in Fig.1A	Species	Accession number	Reference
(1)	*Macrobrachium rosenbergii*	BAB69831	[23]
(2)	*Pandalus hypsinotus*	BAD11098	[42]
(3)	*Homarus americanus*	ABO09863.1	[43]
(4)	*Cherax quadricarinatus*	AAG17936	[3]
(5)	*Upogebia major*	BAF91417.1	[44]
(6)	*Callinectes sapidus*	ABC41925.1	[41]
(7)	*Portunus trituberculatus*	AAX94762.1	[45]
(8)	*Charybdis feriatus*	AAU93694	[46]
(9)	*Scylla serrata*	ACO36035	Chen *et al*. (unpublished)
(10)	*Metapenaeus ensis*	AAN40700	[47]
(11)	*Fenneropenaeus chinensis*	ABC86571.1	[48]
(12)	*Penaeus semisulcatus*	AAL12620	[49]
(13)	*Penaeus monodon*	ABB89953	[50]
(14)	*Litopenaeus vannamei*	AAP76571	[40]
(15)	*Marsupenaeus japonicus*	BAB01568	[51]
(16)	*Fenneropenaeus merguiensis*	AAR88442	[39]

pieces were dehydrated with 100% ACN and dried by vacuum centrifugation (SpeedVac). The *N*-glycans were digested in the gel with PNGase F. Glycans were released with nano-pure water followed by 100% ACN. This procedure was repeated three times. For MALDI-TOF-MS analysis, the glycans were desalted using graphitized carbon. For *N*-glycan sequencing, glycans were labeled with 2-aminobenzamide (2AB) by reductive amination and separated by normal phase HPLC, with a low salt buffer system [29]. The system was calibrated using an external standard of hydrolyzed, 2AB-labelled glucose oligomers to produce a dextran ladder from which the retention times of the individual glycans were converted into glucose units (GU). These GU values were compared with a database of experimental values to obtain preliminary assignments for the glycans. The glycan sequence was obtained by means of glycan digestion. The enzymes used were: GII (goat liver GII, prepared in-house), which cleaves the non-reducing terminal glucose α 1–3 attached to mannose or glucose, and JBM, which cleaves the nonreducing terminal mannose α 1–2, 3, and 6 linkages.

Liquid chromatography and mass spectrometry

To identify the glycosylation sites, the Vg was digested in solution. First, the Vg was reduced and alkylated as described above. Thereafter, Vg was incubated at 37°C with trypsin in 40 mM NH_4HCO_3 with 10% ACN overnight. The tryptic digest was separated using RP-HPLC equipped with a C-18 column (LiChroCART® 250-4 LiChrospher® 100 RP-18 (5 µm), Merck), and the peptides were eluted with the following solutions: Buffer A was composed of 0.1% trifluoroacetic acid (TFA), buffer B was composed of 60% ACN in 0.1% TFA in nano-pure water. A linear gradient of 20–100% of buffer B was created over 60 min at flow rate of 1 ml/min. Fractions of 1 ml were collected and dried by speed vacuum centrifuge and reconstituted with 50% ACN, 0.1% TFA solution containing α-cyano-4-hydroxycinnamic acid (Sigma-Aldrich). The mixture of peptides and matrix solution was spotted on a MALDI target. The fractions of peptides that were detected with the MALDI-TOF and thought to possess a glycan moiety were deglycosylated as described above, and spotted on MALDI target for further analysis. For MS/MS the deglycosylated peptides were reconstituted with 50% ACN, 0.5% formic acid and injected offline.

MALDI-TOF-MS and electrospray ionization MS/MS analysis

Positive ion mode mass spectra were acquired using the MALDI-TOF Bruker Reflex III instrument equipped with delayed extraction (Bruker Daltonik, Bremen, Germany). The acceleration voltage was 20 kV, the pulse voltage was 3200 V. α-Cyano-4-hydroxycinnamic acid (10 mg/ml) in 50% ACN and 0.1% TFA were used as matrix for peptides analysis; 2,5-dihydroxybenzoic acid (Bruker) (10 mg/ml) in 50% ACN and 0.1%TFA was used as matrix for glycan analysis. Conventional and tandem MS for the 139–181 peptides were performed on an orthogonal hybrid quadruple time-of-flight mass spectrometer (Q-TOF, Waters-Micromass) fitted with a Micromass Zspray ion source. Tandem MS was performed by collision induced dissociation (CID) at low energy, using argon as a collision gas. The collision energy was adjusted to that appropriate to the mass of the ions being fragmented, typically between 25 and 45 eV. Data acquired by the Q-TOF

mass spectrometer were processed with a MassLynx data system. LC-MS on a LTQ-Orbitrap was also performed to identify sites of glycosylation of the mixture of deglycosylated peptides. Peptides were resolved by reversed-phase chromatography on 0.075 internal diameter 200 mm length fused silica capillaries (J&W) packed with Reprosil C18 reversed phase beads. The peptides were eluted with linear 75-min gradients, of 5–45%, and 15 min at 95% ACN with 0.1% formic acid in water at a flow rate of 0.25 μL/min. Mass spectrometry was performed with an Orbitrap mass spectrometer (Thermo-Fisher, San Jose) in a positive mode using a repetitive full MS scan followed by CID. The mass spectrometry data was analyzed manually for the presence of deglycosylated peptides.

Results

Bioinformatics analysis and comparison of glycosylation sites from different vitellogenins

The putative glycosylation sites of the deduced amino acid sequence of the Vgs from 16 decapod crustaceans were examined (Fig. 1A). In the *M. rosenbergii* Vg sequence, there are seven putative *N*-glycosylation sites found at N^{151}, N^{159}, N^{168}, N^{614}, N^{660}, N^{1841} and N^{2300} (Fig. 1A, lane 1). The bioinformatics prediction score for *N*-glycosylation of the putative N^{1841} site was negative, while the bioinformatics prediction score for the other six confirmed glycosylation sites were positive. Based on the bioinformatics analysis, the 16 crustacean species can be divided into two major groups: a group rich in putative *N*-glycosylation sites, which includes *M. rosenbergii* (Fig. 1, A, Pleocyemata), and a group almost without both putative *N*-glycosylation sites and mucin-type *O*-glycosylation sites (Fig. 1, A, Dendrobranchiata). Two conserved *N*-glycosylation sites were found in the group rich in putative *N*-glycosylation sites ($N^{159/160}$ and N^{660}; Fig. 1, A, Pleocyemata).

Lectin blotting of Vg

Three major Vg subunits are present in the hemolymph of *M. rosenbergii*, with apparent molecular weights of 79 kDa (subunit A), 110 kDa (subunit B) and 89 kDa (subunit C/D). A 199 kDa band, which composed of both B and C/D subunits, can be also detected (Fig. 2). The A and C/D subunits overlap on SDS-PAGE, and visualize as the 89-kDa band(s) (Fig. 2). Staining of the oligosaccharides with a DIG detection kit revealed that the 89 kDa band(s) may possess oligosaccharide moieties. The 89 kDa band(s) exhibited a strong interaction with GNA, which specifically recognizes highly mannosylated oligosaccharides (Fig. 2). The 89-kDa band(s) also exhibited a weak reaction with PNA, which

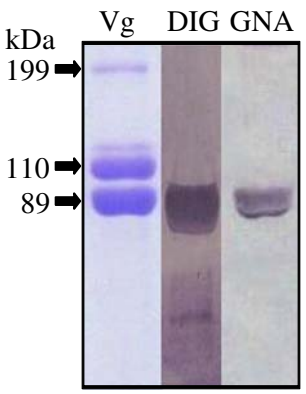

Fig. 2 Oligosaccharide immunoblot detection of hemolymphatic proteins from vitellogenic females and lectin immunoreactivity: Vg — SDS-PAGE of *M. rosenbergii* vitellogenin; DIG — oligosaccharide immunoblot detection; GNA — specific for high mannose glycan chains. The 199 kDa correspond to the B-C/D subunit, 110 kDa correspond to the B subunit and 89 kDa correspond to the A and C/D subunits

recognizes the *O*-glycosylation core disaccharide Galβ (1–3) GalNAc and DSA which, recognizes Galβ(1–4)GlcNAc in either *O*-glycans or in complex and hybrid *N*-glycans (data not shown). No interaction was found with SNA and MAA, which specifically recognize sialic-acid-linked α(2–6) or α(2–3) to galactose, respectively (data not shown).

Mass spectrometry of *N*-glycans

PNGase F-released *N*-linked oligosaccharides from the 89-kDa band(s) were analyzed by using MALDI-TOF-MS. Monoisotopic $[M+Na]^+$ quasi ions at *m/z* of 1582.0, 1744.1, 1906.2 and 2068.3 were detected (Fig. 3). The 162-Da spacing of the ions is indicative of hexose units; hexose-type glycan structures [$Hex_{7/8/9/10}HexNAc_2$, respectively] can be deduced from the monoisotopic masses. The 1906.2 and the 2068.3 *m/z* peaks were the most prominent glycan peaks released from the 89-kDa band(s) (Fig. 3). At a low, but significant, level a $[M+Na]^+$ quasi ion peak having 2230.3 *m/z* — equivalent to the mass of [$Hex_{11}HexNAc_2$] — was also detected in the mass spectrum of the oligosaccharides released from the 89-kDa band(s) by PNGase F. Potassium

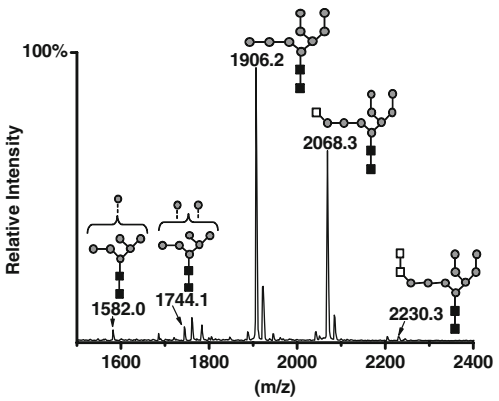

Fig. 3 MALDI mass spectra of oligosaccharides released from the 89-kDa band(s) of *M. rosenbergii* Vg by PNGase F treatment, after in-gel trypsin digestion. Masses indicate monoisotopic $[M+Na]^+$ quasi ions. Schematic representation of the oligosaccharides is included. Black squares — GlcNAc; grey circles — mannose; hollow squares — glucose

adduct $[M+K]^+$ peaks of the same glycans can also be seen to the right of the assigned $[M+Na]^+$ peaks (Fig. 3).

Structural characterization of oligosaccharides

The *N*-linked glycans released from the native protein form and from the 89 kDa band(s) by PNGase F and labeled with 2AB were subjected to normal phase-HPLC, and their GU values were calculated according to dextran standards. The chromatogram showed two prominent peaks, one at 9.49 GU and the other at 10.10 GU (Fig. 4, "Native and 89" panel) and another peak at 8.66 that released from the native protein form (Fig. 4, "Native" panel). The retention times of the peaks were equivalent to $Man_9GlcNAc_2$ (9.49 GU), $Glc_1Man_9GlcNAc_2$ (10.10 GU) and $Man_8GlcNAc_2$ (8.66 GU). GII and JBM were used for further elucidation of the oligosaccharide structure. In response to GII treatment, the peak at 10.10 GU disappeared, but the peak at 9.49 GU remained intact (Fig. 4, "GII" panel). After JBM treatment, both original prominent peaks (10.10 and 9.49 GU) disappeared, and two new peaks appeared at 6.87 and 5.94 GU (Fig. 4, "JBM" panel). The retention times of the two new peaks were equivalent to $Glc_1Man_5GlcNAc_2$ and $Glc_1Man_4GlcNAc_2$, respectively. Combined treatment with GII and JBM led to the complete disappearance of the 10.20 and 9.54 GU peaks (Fig. 4, "GII+JBM" panel).

Identification of glycosylation sites

On the basis of the bioinformatics prediction of putative *N*-glycosylation sites, it was expected that five possible glycopeptides would be present in a virtual tryptic digest of *M. rosenbergii* Vg. MALDI-TOF analysis of the C-18 purified Vg peptides revealed fractions that probably contained glycopeptides and could be assigned to the *M. rosenbergii* Vg sequence (Fig. 5). The spectra of these glycopeptides showed a difference between adjacent peaks of 162-Da, which is equivalent to the mass of one hexose unit. The spectrum of one glycopeptide exhibited three prominent peaks at 9885.5, 10047.0, and 10211.0 *m/z* (Fig. 5A). The peak at 10211.0 *m/z* corresponds to the glycopeptide (139–181 residues) obtained after trypsin

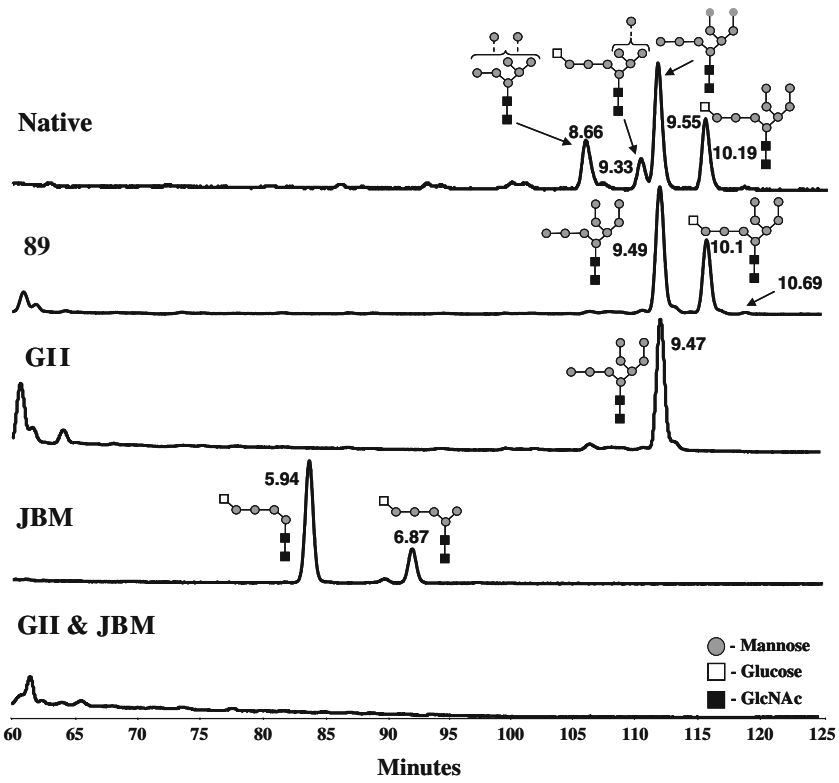

Fig. 4 Normal phase-HPLC chromatogram of glycans released from the native form of Vg and from the 89-kDa band(s) (A and C/D subunits) of SDS-PAGE. Native — the chromatogram shows the intact glycans $Glc_1Man_9GlcNAc_2$, $Glc_1Man_8GlcNAc_2$, $Man_9GlcNAc_2$ and $Man_8GlcNAc_2$ released from the native Vg; 89 — the chromatogram shows the intact oligomannose glycans $Glc_1Man_9GlcNAc_2$ and $Man_9GlcNAc_2$ released from the 89-kDa band(s); GII — the chromatogram shows that the only oligosaccharide remained after GII digestion of the 89 released glycans is $Man_9GlcNAc_2$; JBM — the chromatogram obtained after JBM digestion, indicates that the digestion products are $Glc_1Man_5GlcNAc_2$ and $Glc_1Man_4GlcNAc_2$; GII&JBM — combined digestion of GII followed by JBM. Glucose units of the oligosaccharides are indicated above the peaks. Molecular representation of the oligosaccharides is included. Black squares — GlcNAc; grey circles — mannose; hollow squares — glucose

digestion. The predicted mass of this peptide was 4621.03 Da. The peptide sequence contained three putative *N*-glycosylation sites, and the difference between the predicted mass and the observed mass was 5590 Da, which corresponds to the mass of three $Hex_9GlcNAc_2$ structures (Fig. 5A left). After deglycosylation treatment with PNGase F, the large masses disappeared, and two new peaks emerged at 4678.5 and 4806.5 *m/z*. The 4678.5 *m/z* peak corresponds to the alkylated (57 Da) 139–181 residue sequence of *M. rosenbergii* Vg (Fig. 5A middle). An additional 3 Da accounts for the conversion of asparagine to aspartic acid due to the PNGase F cleavage. The 4806.5 *m/z* peak corresponds to miss-cleavage of a lysine (128 Da) (Fig. 5A middle). The JBM treated glycopeptide revealed a

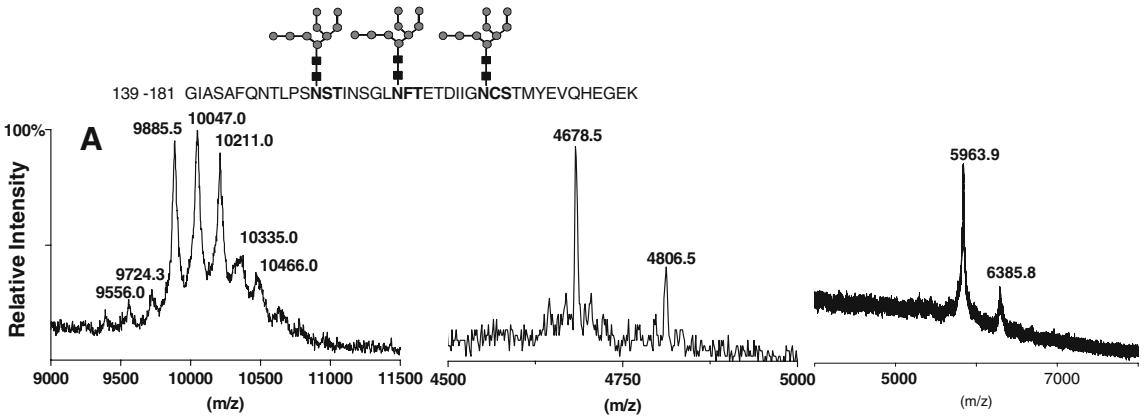

Expected m/z : $[y_{33}\ 1224.9]^{+++}$ $[y_{23}\ 1351.6]^{++}$ $[y_{14}\ 856.3]^{++}$

GIASAFQNTL[PS**N+1**STINSGL **N+1**F TETDIIG **N+1**CSTMYEVQHEGEK

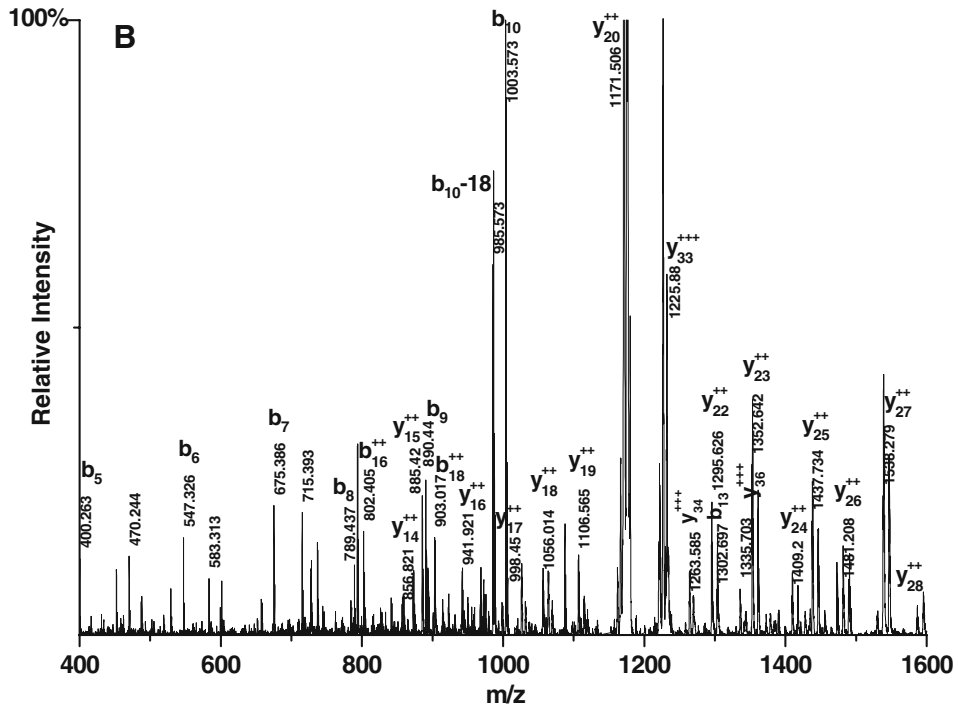

Fig. 5 Glycosylation site identification using MALDI and ESI-MS. **A** Left — MS spectrum of the intact glycopeptide 139–181 amino acid residues, glycosylated at N^{151}, N^{159} and N^{168}; numbers above the peaks represent $[M+H^+]$ of the glycopeptide with different numbers of hexoses. Middle — MS spectrum of the glycopeptide after PNGase F treatment. Right — MS spectrum of the glycopeptide after JBM treatment. Molecular representations of the sugars are indicated. Black squares — GlcNAc; grey circles — mannose. **B** LC-ESI-MS/MS spectrum of 1170.3^{4+} $[M+4H]^{4+}$ ion of the 139–181 amino acid residues after PNGase F treatment. A 1-Da mass gain of Asn after PNGase F treatment is represented by the b and y series ions; y_{14}, y_{24} and y_{33} are specifically indicated in the fragment profile and on peptide sequence at the top of the figure. $^{++}$ and $^{+++}$ indicate doubly and triply charged ions, respectively

prominent peak at 5963.9 corresponds to the lysine miss cleavage in addition to three time the mass of $GlcNac_2$ (3 × 406 Da) (Fig. 5A right) . Additional peak at 6385.8 Da is account for the alkylated and $GlcNAc_2Man_1$ attached to the three asparagines positions of the 139-181 glycopeptides (Fig. 5A right). The ESI-MS analysis of the deglycosylated peptide revealed an ion mass of $[1170.3]^{4+}$. As stated above, the mass $[1170.3, M+4H]^{4+}$, which is equivalent to 4677.2 Da, is 3 Da more than 4674.2 Da, the theoretical mass of amino acid residues 139–181 (Fig. 5B). Tandem MS fragmentation of the deglycosylated $[1170.3]^{4+}$ m/z peptide revealed the typical b and y series ions of the peptides composed of 139–181 amino acid residues of *M. rosenbergii* Vg. The mass shift obtained by deglycosylation with PNGase F is reflected in the b and y series ions: b_{13} has a mass higher by 1 Da than the expected nonglycosylated asparagine, which indicates that N^{151} is glycosylated (Fig. 5B). The 1 Da mass shift of each of the y series ions, specifically y_{14}, y_{23} and y_{33}, provides evidences of glycosylation of N^{151}, N^{159} and N^{168}, respectively (Fig. 5B, see additional details in supplementary data table II).

The spectrum of another glycopeptide exhibited two prominent peaks, 5052.8 and 4889.6*m/z* (Supplementary data figure 4). The 4889.6*m/z* peak corresponds to a C-terminal peptide of 2294–2320 residues (3019.56 Da) attached to a glycan moiety of $Man_9GlcNAc_2$ (1864 Da). The 5052.8*m/z* peak may also corresponds to the same peptide, but is attached to a $Glc_1Man_9GlcNAc_2$ (2026 Da) moiety. This peptide possessed one putative *N*-glycosylation site at N^{2300}. After deglycosylation with PNGase F, a new peak at 3020.1*m/z* was found (Supplementary data figure 4). This peak corresponds to the theoretical peptide mass (3019.56 Da). An oxygen adduct (15.999 Da) at 3036.2*m/z* was also present on this methionine-containing peptide. Tandem MS fragmentation of the deglycosylated peptide revealed the typical b and y series ions for the 2294–2320 residues, with a 1-Da mass gain for b and y fragment ions that contain N^{2300} (Supplementary data figure 4). Additionally, the glycosylation of N^{614} and N^{660} was confirmed using LC-MS/MS analysis (Table 2 and Supplementary data figures 2–3). However, the putative *N*-glycosylation N^{1841} site was not confirmed: it was not evident in the spectra of the intact or deglycosylated peptides.

Discussion

Although the structure and function of the *N*-glycan moieties of proteins have been studied intensively, the structure of the glycan moieties of crustacean Vgs and their function have not yet been elucidated. In the present study, the putative *N*- and *O*-glycosylation sites of deduced Vg sequences from 16 decapod crustacean species were predicted bioinformatically. The analysis revealed a clear segregation of the 16 species into two different crustacean groups (see Fig. 1 and Table 1). One group, the Pleocyemata, is rich in putative *N*-glycosylation sites and also possesses *O*-glycosylation sites (Fig. 1, Pleocyemata), whereas the other group, the Dendrobranchiata, exhibits a remarkable deficiency in putative *N*-glycosylation sites (Fig. 1, Dendrobranchiata). This segregation resembles the natural taxonomic segregation and differences in female reproductive strategy, in that the Pleocyemata are egg-holding species, while the Dendrobranchiata are egg-releasing species. It thus seems that there is a strong selective force against the occurrence of *N*-glycosylation sites in the Dendrobranchiata suborder. This segregation of glycosylation sites may shed light on biochemical characteristics of Vg and may thus explain the different reproductive strategies of the two groups. The Vg of *M. rosenbergii*, which belongs to the suborder Pleocyemata, possesses seven putative *N*-glycosylation sites and another single mucin-type *O*-glycosylation site. The treatment of this Vg with GNA indicated the presence of *N*-glycosylation of the high mannose type (Fig. 2); this finding is consistent with the common glycosylation of arthropod glycoproteins, such as the hemocyanin of *Astacus leptodactylus* [30], the hemoglobins of the deep-sea tube worm *Riftia pachyptila* [31], the larval serum protein of *Drosophila melanogaster* [32], and the storage glycoprotein, arylphorin, of lepidopteran insects [20, 33]. As was to be expected, no interaction was found with either of the sialic-acid-specific lectins, SNA and MAA. To date, sialic acid has not been detected in arthropod glycoproteins, and thus the absence of sialic acid residues in crustacean Vg is consistent with the glycan moieties composition of arthropod Vgs. The fact that GNA detected only the 89 kDa band(s) is not surprising. As stated above, the 89 kDa band(s) contains both the A and the C/D subunits from the *N*-terminus and the *C*-terminus, respectively. The glycosylation of these two subunits was confirmed by the identification of glycosylation sites. The B-C/D subunit (199 kDa) (Fig. 2) is supposed to be glycosylated, however its low level in the SDS-PAGE might be under the detection limit and thus not detected by GNA.

In line with the GNA immunoblotting (Fig. 2), mass spectrometry glycan analysis revealed a spectrum containing high-hexose oligosaccharides ($Hex_{7\text{-}11}HexNAc_2$) (Fig. 3). Exoglycosidase sequencing revealed that the glycan moieties of *M. rosenbergii* Vg are composed of high mannose oligosaccharides ($Man_9GlcNAc_2$) and a glucose-capped high mannose oligosaccharide ($Glc_1Man_9GlcNAc_2$). Oligosaccharide structures correspond to $Man_9GlcNac_2$ and $Glc_1Man_8GlcNAc_2$ were detected in the chromatogram of glycan released from the native protein (Fig. 4, native). Minute amount of the $Man_8GlcNAc_2$ form was also detected in glycans released from the 89 kDa band(s) by in gel digestion (Fig. 4, 89). For

Table 2 Glycopeptide masses and identified site of glycosylation of *M. rosenbergii* vitellogenin

Peptide	Glycopeptide[a] mass	Deglycosylated peptide mass	Nonglycosylated expected mass	Glycosylation sites
139–189	10211.0	4678.6	4675.2	N^{151}, N^{159}, N^{168}
	10047.0			
	9885.5			
606–617	3428.5	1362.8	1361.8	N^{614}
656–678	N.D[b]	2300.28	2299.24	N^{660}
2294–2320	4889.6	3020.1	3019.6	N^{2300}
	5052.8			

[a] glycoform masses observed in MALDI and ESI-MS analysis

[b] N.D=not detected

native glycan digestion a larger amount of Vg was used. The abundance of $Man_8GlcNAc_2$ and $Glc_1Man_8GlcNAc_2$, could be attributed to the quantity of the digested glycoprotein or as a result of degradation due to prolonged storage period. Moreover, in this study, a unique doubly glucosylated high mannose structure was shown for the first time (Fig. 4). Highly mannosylated glycoforms have also been detected in Vg from the crab *Callinectes sapidus* (see Supplementary figure 1 and table I) and in Vg from *Cherax quadricarinatus* [14] (see Supplementary table I). Unique glucose-capped glycoforms have also been detected in several other proteins, such as the avian immunoglobulin IgY and human IgE [16–19] and in storage proteins like arylphorin of the silk worm *Antheraea pernyi* [20] and the egg jelly coat of the starfish, *Asterias amurensis* [21]. Endo *et al.* (1987) [21] suggested that the presence of monoglucosylated oligosaccharides is due to the low activity of the enzyme GII in these animals. Deprez *et al.* (2005) [34] posited that adjacent or multi *N*-glycan moieties are advantageous for GII trimming activity, and thus glucose caps would not be found on *N*-linked oligosaccharide chains of a multi *N*-glycosylated protein. We would therefore not expect to find glucose caps on the Vg of *M. rosenbergii* [with five *N*-glycosylated sites at the N-terminus domain (N^{151}, N^{159}, N^{168}, N^{614}, N^{660}) and another site at the C-terminus (N^{2300})] (Fig. 5, 6, Table 2 and Supplementary data) or on the Vg of *Cherax quadricarinatus* [with adjacent *N*-glycan moieties at the N-terminus (N^{152}, N^{160}) and an *N*-glycan moiety at the C-terminus N^{2493}] [14]. Nevertheless, glucose-capped *N*-linked oligosaccharides were found in both the Vgs of *M. rosenbergii* and *Cherax quadricarinatus* [14].

A 3D model of avian IgY predicted that the monoglucosylated glycans face the interior side of the antibody, and this may explain the inaccessibility of the glycan moiety to further trimming by GII [35]. In *M. rosenbergii*, the three *N*-glycosylated sites of Vg (N^{151}, N^{159} and N^{168}) are located in the lipoprotein domain (Fig. 1B). Noteworthy that in pleocyemata crustaceans the putative *N*-glycosylation (N^{160}) is a conserved site. The theoretical 3D model illustrates that the three *N*-terminal asparagine residues (N^{151}, N^{159} and N^{168}) are exposed to the outer surface of the polypeptide structure (Fig. 6). Additionally, glycan moieties cleaved with PNGase F, from the native form of Vg, revealed that the released glycans were composed of highly mannosylated and glucose-capped oligosaccharides (Fig. 4, "Native" panel). In contrast to the previous findings, for avian IgY [34], arylphorin [20], jack bean α-mannosidase [36], and bovine lysosomal α-mannosidase [37, 38], the *N*-glycan moieties of *M. rosenbergii* Vg might be accessible to the trimming activity of GII. However, the 3D model is not the ultimate evidence that the sites are really exposed;

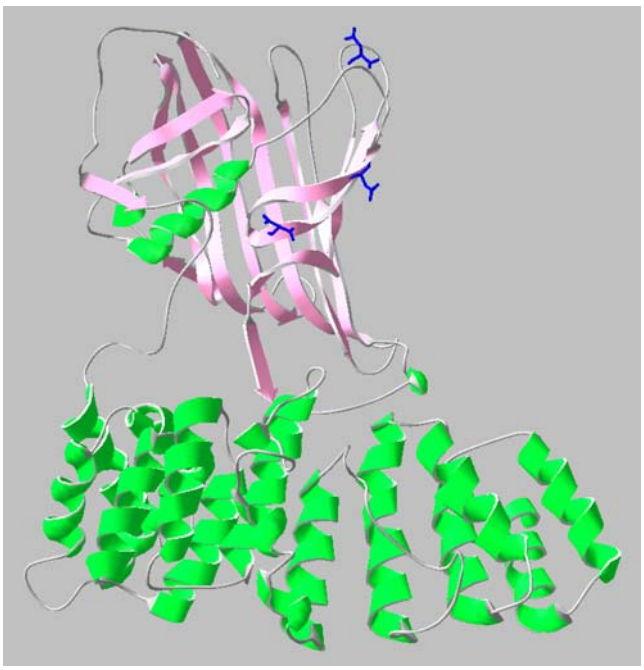

Fig. 6 3D model of the lipoprotein domain of Vg from *M. rosenbergii*, based on the lipoprotein domain of the silver lamprey (PDB 1LSH). The 3D model was constructed by the ESyPred3D Webserver and processed by Swiss-PdbViewer software. The three glycosylated asparagine residues (N^{151}, N^{159} and N^{168}) are exposed to the outer environment

still it may provide some clues for the accessibility by glucosidase II in the ER. A support for the glucose trimming of the N-terminally exposed sites can be seen from the JBM treatment of this specific glycocopeptide (Fig. 5). The glycan moieties on Vg might contribute to the solubility of this hydrophobic protein and thereby facilitate the transport of Vg in the hemolymph.

The expression rate of the studied proteins may explain the presence of a glycan moiety bearing a glucose cap. Glycoproteins such as arylphorin and Vg are fast-accumulating proteins. Vg is over-expressed through the process of vitellogenesis, and its levels decline shortly afterwards [39–41]. Immunoglobulins are over-expressed as a result of immunological stress or due to maternal care, as seen in yolk IgY. Therefore, we suggest that over-expressed proteins, such as those mentioned above, may overwhelm the quality-control glycosylation machinery. Thus, the trimming process of the glycan moiety cannot cope with large amount of glycoproteins, and consequently glucose-capped glycan moieties are found. The above suggestion is supported by the presence of different glycoforms of the same glycoprotein. Future work is needed to confirm the above hypothesis and to elucidate the general role of the glycan moieties in crustacean Vgs and specifically the importance of these *N*-glycosylation conserved sites. Understanding structure and modifications of Vg, as a key protein in embryonic development, and the regulatory factors that control translation, secretion and accumulation of Vg are important issues for aquaculture and for pest control, specifically of invertebrate species.

Acknowledgments We thank Ayana Benet-Perlberg and the team from the Dor experimental station of the Ministry of Agriculture for providing animal culture facilities, Mr. Tomer Ventura for his technical assistance and Ms. Lilah Glazer for her help in generating the 3D model. This work was supported by an internal grant from Ben Gurion University of the Negev; I. K. is the incumbent of MAOF fellowship from the Israel Council for Higher Education, Planning and Budgeting Committee.

References

1. Tata, J.R.: Coordinated assembly of the developing egg. Bio-Essays **4**, 197–201 (1986)
2. Pan, M.L., Bell, W.J., Telfer, W.H.: Vitellogenic blood protein synthesis by insect fat body. Science **165**, 393–394 (1969)
3. Abdu, U., Davis, C., Khalaila, I., Sagi, A.: The vitellogenin cDNA of *Cherax quadricarinatus* encodes a lipoprotein with calcium binding ability, and its expression is induced following the removal of the androgenic gland in a sexually plastic system. Gen. Comp. Endocrinol. **127**, 263–272 (2002)
4. Chen, Y.N., Tseng, D.Y., Ho, P.Y., Kuo, C.M.: Site of vitellogenin synthesis determined from a cDNA encoding a vitellogenin fragment in the freshwater giant prawn, *Macrobrachium rosenbergii*. Mol. Reprod. Dev. **54**, 215–222 (1999)
5. Tseng, D.Y., Chen, Y.N., Kou, G.H., Lo, C.F., Kuo, C.M.: Hepatopancreas is the extraovarian site of vitellogenin synthesis in black tiger shrimp, *Penaeus monodon*. Comp. Biochem. Physiol. A Mol. Integr. Physiol. **129**, 909–917 (2001)
6. Opresko, L.K., Wiley, H.S.: Receptor-mediated endocytosis in Xenopus oocytes. I. Characterization of the vitellogenin receptor system. J. Biol. Chem. **262**, 4109–4115 (1987)
7. Shen, X., Steyrer, E., Retzek, H., Sanders, E.J., Schneider, W.J.: Chicken oocyte growth: receptor-mediated yolk deposition. Cell Tissue Res. **272**, 459–471 (1993)
8. Snigirevskaya, E.S., Sappington, T.W., Raikhel, A.S.: Internalization and recycling of vitellogenin receptor in the mosquito oocyte. Cell Tissue Res. **290**, 175–183 (1997)
9. Warrier, S., Subramoniam, T.: Receptor mediated yolk protein uptake in the crab *Scylla serrata*: crustacean vitellogenin receptor recognizes related mammalian serum lipoproteins. Mol. Reprod. Dev. **61**, 536–548 (2002)
10. Hafer, J., Ferenz, H.J.: Locust vitellogenin receptor — an acidic glycoprotein with *N*-linked and *O*-linked oligosaccharides. Comp. Biochem. Physiol. B-Biochem. Mol. Biol. **100**, 579–586 (1991)
11. Finn, R.N.: Vertebrate yolk complexes and the functional implications of phosvitins and other subdomains in vitellogenins. Biol. Reprod. **76**, 926–935 (2007)
12. Tirumalai, R., Subramoniam, T.: Carbohydrate components of lipovitellin of the sand crab *Emerita asiatica*. Mol. Reprod. Dev. **58**, 54–62 (2001)
13. Wallace, R.A., Walker, S.L., Hauschka, P.V.: Crustacean lipovitellin. Isolation and characterization of the major high-density lipoprotein from the eggs of decapods. Biochemistry **6**, 1582–1590 (1967)
14. Khalaila, I., Peter-Katalinic, J., Tsang, C., Radcliffe, C.M., Aflalo, E.D., Harvey, D.J., Dwek, R.A., Rudd, P.M., Sagi, A.: Structural characterization of the *N*-glycan moiety and site of glycosylation in vitellogenin from the decapod crustacean *Cherax quadricarinatus*. Glycobiology **14**, 767–774 (2004)
15. Ellgaard, L., Molinari, M., Helenius, A.: Setting the standards: Quality control in the secretory pathway. Science **286**, 1882–1888 (1999)
16. Matsuura, F., Ohta, M., Murakami, K., Matsuki, Y.: Structures of asparagine linked oligosaccharides of immunoglobulins (IgY) isolated from egg-yolk of Japanese quail. Glycoconj. J. **10**, 202–213 (1993)
17. Ohta, M., Hamako, J., Yamamoto, S., Hatta, H., Kim, M., Yamamoto, T., Oka, S., Mizuochi, T., Matsuura, F.: Structures of asparagine-linked oligosaccharides from hen egg-yolk antibody (IgY). Occurrence of unusual glucosylated oligo-mannose type oligosaccharides in a mature glycoprotein. Glycoconj. J. **8**, 400–413 (1991)
18. Suzuki, N., Khoo, K.H., Chen, C.M., Chen, H.C., Lee, Y.C.: N-glycan structures of pigeon IgG: A major serum glycoprotein containing Galalpha1–4 Gal termini. J. Biol. Chem. **278**, 46293–46306 (2003)
19. Arnold, J.N., Radcliffe, C.M., Wormald, M.R., Royle, L., Harvey, D.J., Crispin, M., Dwek, R.A., Sim, R.B., Rudd, P.M.: The glycosylation of human serum IgD and IgE and the accessibility of identified oligomannose structures for interaction with mannan-binding lectin. J. Immunol. **173**, 6831–6840 (2004)
20. Kim, S., Hwang, S.K., Dwek, R.A., Rudd, P.M., Ahn, Y.H., Kim, E.H., Cheong, C., Kim, S.I., Park, N.S., Lee, S.M.: Structural determination of the *N*-glycans of a lepidopteran arylphorin reveals the presence of a monoglucosylated oligosaccharide in the storage protein. Glycobiology **13**, 147–157 (2003)
21. Endo, T., Hoshi, M., Endo, S., Arata, Y., Kobata, A.: Structures of the sugar chains of a major glycoprotein present in the egg jelly coat of a starfish, *Asterias amurensis*. Arch. Biochem. Biophys. **252**, 105–112 (1987)
22. Varki, A., Cummings, R., et al.: Essentials of glycobiology. Cold Spring Harbor Laboratory Press, NY (1999)

23. Okuno, A., Yang, W.J., Jayasankar, V., Saido-Sakanaka, H., Huong, D.T., Jasmani, S., Atmomarsono, M., Subramoniam, T., Tsutsui, N., Ohira, T., Kawazoe, I., Aida, K., Wilder, M.N.: Deduced primary structure of vitellogenin in the giant freshwater prawn, *Macrobrachium rosenbergii*, and yolk processing during ovarian maturation. J. Exp. Zool. **292**, 417–429 (2002)
24. Gupta, R., Brunak, S.: Prediction of glycosylation across the human proteome and the correlation to protein function. Pac. Symp. Biocomput., 310–322 (2002)
25. Julenius, K., Molgaard, A., Gupta, R., Brunak, S.: Prediction, conservation analysis, and structural characterization of mammalian mucin-type *O*-glycosylation sites. Glycobiology **15**, 153–164 (2005)
26. Lambert, C., Leonard, N., De Bolle, X., Depiereux, E.: ESyPred3D: Prediction of proteins 3D structures. Bioinformatics (Oxford, England) **18**, 1250–1256 (2002)
27. Guex, N., Peitsch, M.C.: SWISS-MODEL and the Swiss-PdbViewer: An environment for comparative protein modeling. Electrophoresis **18**, 2714–2723 (1997)
28. Abdu, U., Yehezkel, G., Sagi, A.: Oocyte development and polypeptide dynamics during ovarian maturation in the red-claw crayfish *Cherax quadricarinatus*. Invert. Reprod. Develop. **37**, 75–83 (2000)
29. Kuster, B., Wheeler, S.F., Hunter, A.P., Dwek, R.A., Harvey, D.J.: Sequencing of *N*-linked oligosaccharides directly from protein gels: In-gel deglycosylation followed by matrix-assisted laser desorption/ionization mass spectrometry and normal-phase high-performance liquid chromatography. Anal. Biochem. **250**, 82–101 (1997)
30. Tseneklidou-Stoeter, D., Gerwig, G.J., Kamerling, J.P., Spindler, K.D.: Characterization of *N*-linked carbohydrate chains of the crayfish, *Astacus leptodactylus* hemocyanin. Biol. Chem. Hoppe-Seyler **376**, 531–537 (1995)
31. Zal, F., Kuster, B., Green, B.N., Harvey, D.J., Lallier, F.H.: Partially glucose-capped oligosaccharides are found on the hemoglobins of the deep-sea tube worm *Riftia pachyptila*. Glycobiology **8**, 663–673 (1998)
32. Williams, P.J., Wormald, M.R., Dwek, R.A., Rademacher, T.W., Parker, G.F., Roberts, D.R.: Characterisation of oligosaccharides from *Drosophila melanogaster* glycoproteins. Biochim. Biophys. Acta. **1075**, 146–153 (1991)
33. Ryan, R.O., Anderson, D.R., Grimes, W.J., Law, J.H.: Arylphorin from *Manduca sexta*: Carbohydrate structure and immunological studies. Arch. Biochem. Biophys. **243**, 115–124 (1985)
34. Deprez, P., Gautschi, M., Helenius, A.: More than one glycan is needed for ER glucosidase II to allow entry of glycoproteins into the calnexin/calreticulin cycle. Mol. Cell **19**, 183–195 (2005)
35. Suzuki, N., Lee, Y.C.: Site-specific *N*-glycosylation of chicken serum IgG. Glycobiology **14**, 275–292 (2004)
36. Kimura, Y., Hess, D., Sturm, A.: The *N*-glycans of jack bean alpha-mannosidase. Structure, topology and function. Eur. J. Biochem. **264**, 168–175 (1999)
37. Faid, V., Evjen, G., Tollersrud, O.K., Michalski, J.C., Morelle, W.: Site-specific glycosylation analysis of the bovine lysosomal alpha-mannosidase. Glycobiology **16**, 440–461 (2006)
38. Heikinheimo, P., Helland, R., Leiros, H.K., Leiros, I., Karlsen, S., Evjen, G., Ravelli, R., Schoehn, G., Ruigrok, R., Tollersrud, O.K., McSweeney, S., Hough, E.: The structure of bovine lysosomal alpha-mannosidase suggests a novel mechanism for low-pH activation. J. Mol. Biol. **327**, 631–644 (2003)
39. Phiriyangkul, P., Utarabhand, P.: Molecular characterization of a cDNA encoding vitellogenin in the banana shrimp, *Penaeus (Litopenaeus) merguiensis* and sites of vitellogenin mRNA expression. Mol. Reprod. Dev. **73**, 410–423 (2006)
40. Raviv, S., Parnes, S., Segall, C., Davis, C., Sagi, A.: Complete sequence of *Litopenaeus vannamei* (Crustacea: Decapoda) vitellogenin cDNA and its expression in endocrinologically induced sub-adult females. Gen. Comp. Endocrinol. **145**, 39–50 (2006)
41. Zmora, N., Trant, J., Chan, S.M., Chung, J.S.: Vitellogenin and its messenger RNA during ovarian development in the female blue crab, *Callinectes sapidus*: Gene expression, synthesis, transport, and cleavage. Biol. Reprod. **77**, 138–146 (2007)
42. Tsutsui, N., Saido-Sakanaka, H., Yang, W.J., Jayasankar, V., Jasmani, S., Okuno, A., Ohira, T., Okumura, T., Aida, K., Wilder, M.N.: Molecular characterization of a cDNA encoding vitellogenin in the coonstriped shrimp, *Pandalus hypsinotus* and site of vitellogenin mRNA expression. J. Exp. Zoolog. A Comp. Exp. Biol. **301**, 802–814 (2004)
43. Tiu, S.H., Hui, H.L., Tsukimura, B., Tobe, S.S., He, J.G., Chan, S.M.: Cloning and expression study of the lobster (*Homarus americanus*) vitellogenin: Conservation in gene structure among decapods. Gen. Comp. Endocrinol. **160**, 36–46 (2009)
44. Kang, B.J., Nanri, T., Lee, J.M., Saito, H., Han, C.H., Hatakeyama, M., Saigusa, M.: Vitellogenesis in both sexes of gonochoristic mud shrimp, *Upogebia major* (Crustacea): Analyses of vitellogenin gene expression and vitellogenin processing. Comp. Biochem. Physiol. B Biochem. Mol. Biol. **149**, 589–598 (2008)
45. Yang, F., Xu, H.T., Dai, Z.M., Yang, W.J.: Molecular characterization and expression analysis of vitellogenin in the marine crab *Portunus trituberculatus*. Comp. Biochem. Physiol. B Biochem. Mol. Biol. **142**, 456–464 (2005)
46. Mak, A.S., Choi, C.L., Tiu, S.H., Hui, J.H., He, J.G., Tobe, S.S., Chan, S.M.: Vitellogenesis in the red crab *Charybdis feriatus*: Hepatopancreas-specific expression and farnesoic acid stimulation of vitellogenin gene expression. Mol. Reprod. Dev. **70**, 288–300 (2005)
47. Tsang, W.S., Quackenbush, L.S., Chow, B.K., Tiu, S.H., He, J.G., Chan, S.M.: Organization of the shrimp vitellogenin gene: Evidence of multiple genes and tissue specific expression by the ovary and hepatopancreas. Gene **303**, 99–109 (2003)
48. Xie, S., Sun, L., Liu, F., Dong, B.: Molecular characterization and mRNA transcript profile of vitellogenin in Chinese shrimp, *Fenneropenaeus chinensis*. Mol. Biol. Rep. (2007)
49. Avarre, J.C., Michelis, R., Tietz, A., Lubzens, E.: Relationship between vitellogenin and vitellin in a marine shrimp (*Penaeus semisulcatus*) and molecular characterization of vitellogenin complementary DNAs. Biol. Reprod. **69**, 355–364 (2003)
50. Tiu, S.H., Hui, J.H., He, J.G., Tobe, S.S., Chan, S.M.: Characterization of vitellogenin in the shrimp *Metapenaeus ensis*: Expression studies and hormonal regulation of MeVg1 transcription in vitro. Mol. Reprod. Dev. **73**, 424–436 (2006)
51. Tsutsui, N., Kawazoe, I., Ohira, T., Jasmani, S., Yang, W.J., Wilder, M.N., Aida, K.: Molecular characterization of a cDNA encoding vitellogenin and its expression in the hepatopancreas and ovary during vitellogenesis in the kuruma prawn, *Penaeus japonicus*. Zool. Sci. **17**, 651–660 (2000)